Supporting Information

For

Rational Design of 2D Janus $CuFeO_{2+\delta}$ Single-layer as Photocatalyst and Photoelectrode

Zong-Yan Zhao*, Qing-Lu Liu

Faculty of Materials Science and Engineering, Kunming University of Science and Technology, Kunming 650093, People's Republic of China

* E-mail: zzy@kust.edu.cn

1. Structure and morphology of as-prepared samples

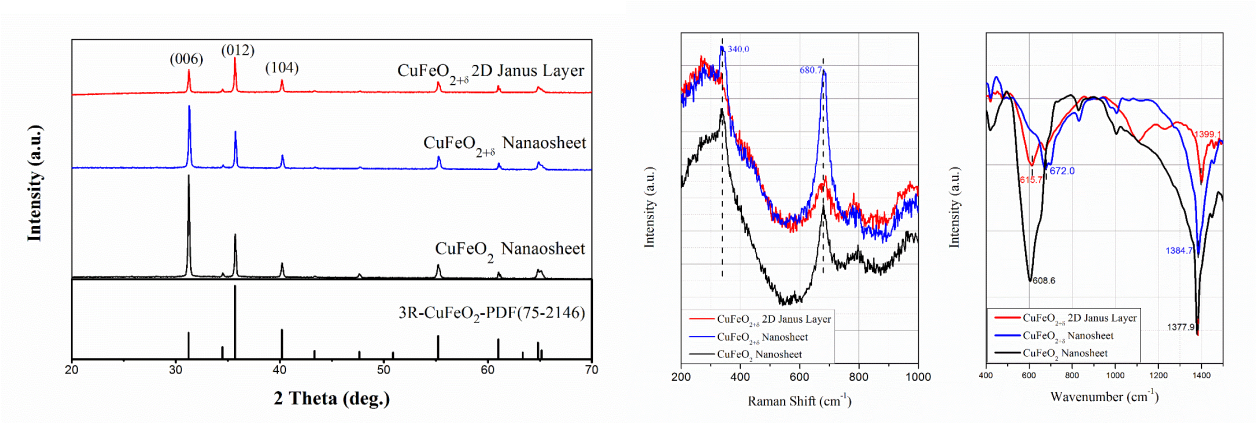

Figure S1. XRD patterns, Raman and FTIR spectra of as-prepared $CuFeO_2$ Nanosheet, $CuFeO_{2+\delta}$ Nanosheet and $CuFeO_{2+\delta}$ 2D Janus Layer samples

Figure S1(a) is the XRD pattern of $CuFeO_2$ nanosheet, $CuFeO_{2+\delta}$ nanosheet and $CuFeO_{2+\delta}$ 2D Janus Layer. The diffraction peaks of the three groups of samples are consistent with the standard diffraction peak of delafossite 3R-$CuFeO_2$ (JCPDS 75-2146). Among them, the difference is that the main diffraction peak of $CuFeO_2$ nanosheet and $CuFeO_{2+\delta}$ nanosheet becomes the diffraction peak of the (006) crystal plane, which is due to the characteristics of nanosheet exhibited after preferential growth. This is due to the fact that the hydrothermal synthesis process has been optimized and the sample has been selectively grown, so that the (006) surface becomes the primary crystal surface.

Figure S1(b) is the Raman spectrum and FTIR spectrum of $CuFeO_2$ nanosheet, $CuFeO_{2+\delta}$ nanosheet and $CuFeO_{2+\delta}$ 2D Janus Layer. For the Raman spectrum, in addition to the features

analyzed in our previous reports,[1-2] the most prominent feature is that the diffraction peak of the $CuFeO_{2+\delta}$ 2D Janus Layer sample is significantly broadened compared to the other two samples. This is due to the introduction of a certain amount of 2D Janus $CuFeO_{2+\delta}$ single-/few-layer in the sample reduce the crystallinity of the sample, which is consistent with the results of XRD test. For the FTIR spectrum of $CuFeO_2$ nanosheet and $CuFeO_{2+\delta}$ nanosheet, the vibration peak at 608.6 cm^{-1} disappeared as the excess O content increased. This vibration peak is the characteristic vibration peak of the Cu^{1+} linear coordination O-Cu-O dumbbell structure, indicating that the O-Cu-O dumbbell structure gradually weakens with the introduction of excess O and eventually disappears. In $CuFeO_2$ nanosheet, the 608.6 cm^{-1} peak is contributed by O-Cu-O stretch vibration; while in $CuFeO_{2+\delta}$ nanosheet, the 672 cm^{-1} peak is contributed by $[CuO_4]$ vibration; while in $CuFeO_{2+\delta}$ 2D Janus layer, due to lack the interlayer interaction, this peak is red-shifting in compared with $CuFeO_{2+\delta}$ nanosheet. On the other hand, with the introduction of excessive O, the vibration peak at 1377.9 cm^{-1} caused by the tensile vibration of Fe-O in the twisted $[FeO_6]$ octahedron is gradually blue shifting, indicating that the tensile vibration of Fe-O is strengthening, that is, the Fe-O bond is getting longer. The characteristic vibration peaks of $CuFeO_{2+\delta}$ nanosheet and $CuFeO_{2+\delta}$ 2D Janus Layer sample are exactly the same, with only a slight red shift, which indicates that $CuFeO_{2+\delta}$ has an intrinsic open layered structure, and the microstructures of $CuFeO_{2+\delta}$ 2D Janus Layer sample are basically the same as $CuFeO_{2+\delta}$ nanosheet, which is consistent with the data analysis of Fig. 1(a).

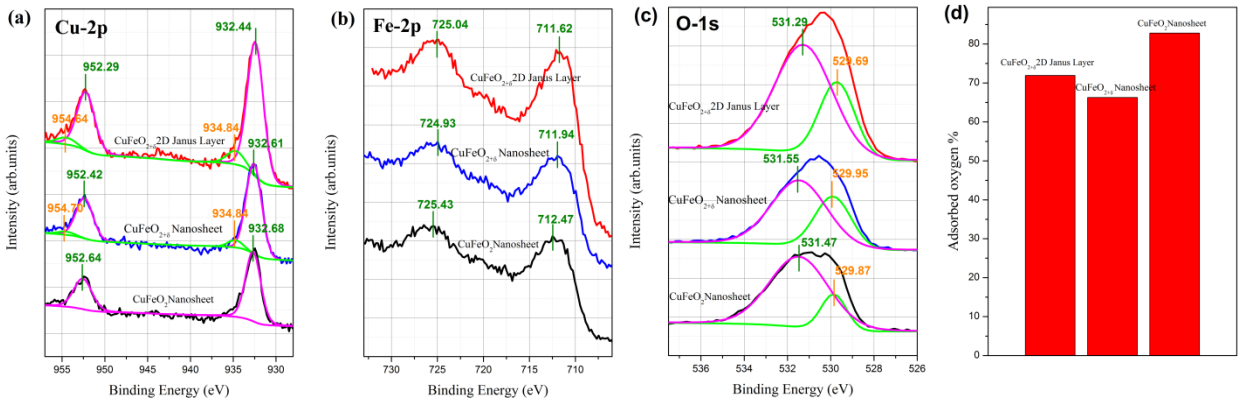

Figure S2. The XPS spectra of as-prepared $CuFeO_2$ Nanosheet, $CuFeO_{2+\delta}$ Nanosheet, and $CuFeO_{2+\delta}$ 2D Janus Layer samples, (a) Cu-2p, (b) Fe-2p, (c) O-1s and (d) the corresponding adsorbed O content

Figure S2 is the XPS spectrum of $CuFeO_2$ nanosheet, $CuFeO_{2+\delta}$ nanosheet and $CuFeO_{2+\delta}$ 2D Janus Layer. The presence of the shoulder peaks at ~934.8 and ~954.6 eV and satellite peaks confirms that the $CuFeO_{2+\delta}$ nanosheet and $CuFeO_{2+\delta}$ 2D Janus Layer samples contained Cu^{2+} ions.[2]

The Fe-2p peaks of these three samples are seen to match Fe^{3+},[3] which indicates that the chemical coordination environment around Fe atoms has not changed significantly, which is consistent with our previous reports.[2] Comparing the Fe-3p peaks of the two samples of $CuFeO_{2+\delta}$ nanosheet and $CuFeO_{2+\delta}$ 2D Janus Layer, it can be seen that $CuFeO_{2+\delta}$ has an intrinsic open layered structure, the interlayer interaction is weak, and the microstructures of $CuFeO_{2+\delta}$ 2D Janus Layer sample are basically the same as $CuFeO_{2+\delta}$ nanosheet, which is consistent with the data analysis in Fig. 1(a) and the FTIR spectrum analysis in Figure S1(b). The adsorbed oxygen can be recognized and calculated by the relative area of peak that is centered at ~529.8 eV in the O-1s XPS spectra. The other peak centered at ~531.4 eV is ascribed to the lattice oxygen.[3] Figure S2(d) shows that $CuFeO_2$ nanosheet has the largest proportion of oxygen adsorbed on surface. This is because the exposed surface of $CuFeO_2$ nanosheet is Cu atoms with hanging bonds, so it is easy to absorb oxygen in the environment. However, the Cu atoms in the exposed surface of $CuFeO_{2+\delta}$ nanosheet and $CuFeO_{2+\delta}$ 2D Janus Layer have bonded with the introduced excess O, so the density of hanging bond is low, which limits the further adsorption of oxygen in the air. Compared to the $CuFeO_{2+\delta}$ nanosheet sample, the adsorbed oxygen content of the $CuFeO_{2+\delta}$ 2D Janus Layer sample is slightly higher, which is due to the increased specific surface area of the sample after being exfoliated (The specific surface areas of $CuFeO_2$ nanosheet, $CuFeO_{2+\delta}$ nanosheet and $CuFeO_{2+\delta}$ 2D Janus Layer are17.33, 46.48, 52.12 m^2/g, respectivly, obtained by the Langmuir method).

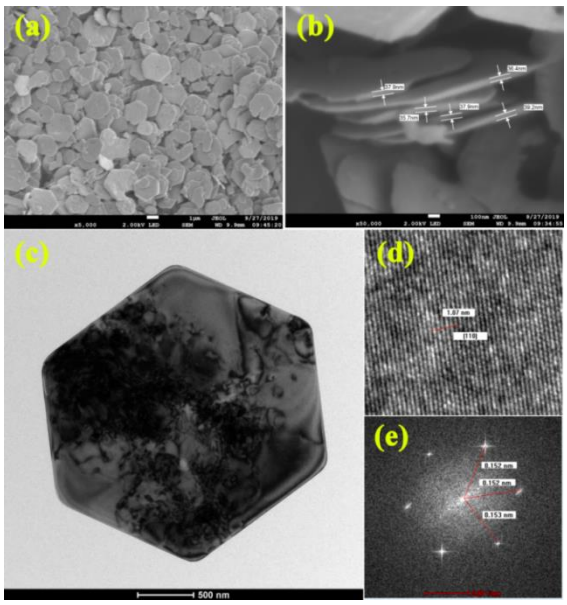

Figure S3. (a) SEM full view image; (b) SEM locally enlarged image with marked thickness; (c) TEM image; (d) High-resolution TEM lattice stripe image; and (e) TEM electron diffraction pattern of as-prepared hexagonal $CuFeO_2$ nanosheet.

Figure S3 shows the SEM images of $CuFeO_2$ nanosheet with hexagonal flake morphology and high crystallinity. The lattice fringes of $CuFeO_2$ samples obtained by high-resolution transmission electron microscopy (HRTEM) along the direction of [110] is basically the same as that of $CuFeO_{2+\delta}$ material (Fig. 3(b)), indicating that the introduction of excess oxygen had little impact on the lattice constants a and b, which is consistent with the theoretical calculation results in our previous report.

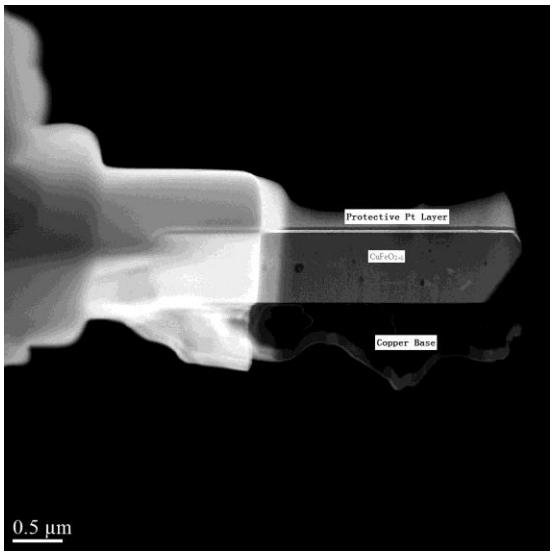

Figure S4. The morphology of $CuFeO_{2+\delta}$ nanosheet obtained by FIB thinning

In order to further prove that the introduction of non-stoichiometric oxygen makes the layered structure of $CuFeO_2$ more prominent, a cross-sectional TEM lamella was prepared from the as-grown single crystal using the focused ion beam (FIB), which was shown in Figure S4.

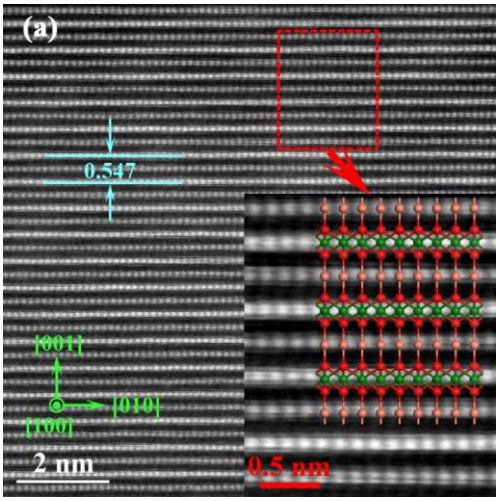

Figure S5. HADDF-STEM image showing the cross section of the $CuFeO_2$ single crystal prepared by FIB. The crystal structure is overlaid, where Cu, Fe, and O atoms are represented by brick red, green, and red circles, respectively

Figure S5 is the high-angle annular dark field scan transmission electron microscopy (HAADF-STEM) image of $CuFeO_2$, which emphasizes the repeating layers of Cu and FeO that looks down on the [001] crystal zone proved the exposure of the (001) crystal surface. It is worth noting that the spacing of $CuFeO_2$ (0.547 nm) between the adjacent Cu atomic layers is smaller than the spacing of $CuFeO_{2+\delta}$ (0.639 nm, Fig. 3(c)), which demonstrates that the presence of excess oxygen can weaken the interlayer interaction in $CuFeO_2$, displaying a layered structure along with weak van der Waals interlayer interaction. This phenomenon is also consistent with the theoretical calculation results in our previous report.

2. Properties of as-prepared samples

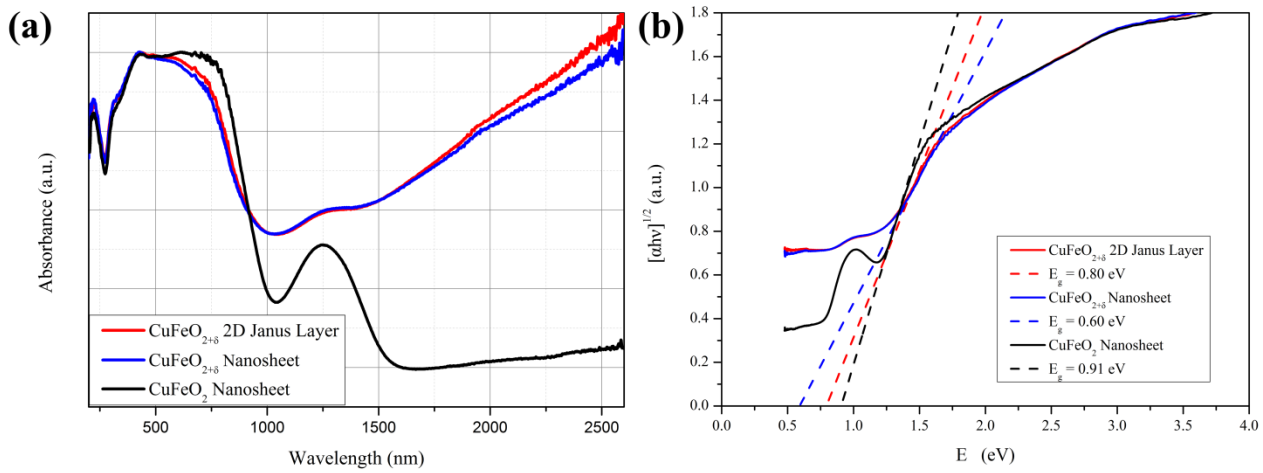

Figure S6. (a) The UV-Vis-NIR DRS spectra and corresponding Kubelka–Munk plots of as-prepared $CuFeO_2$ Nanosheet, $CuFeO_{2+\delta}$ Nanosheet, and $CuFeO_{2+\delta}$ 2D Janus Layer samples

Figure S6 shows the UV-VIS-NIR DRS spectrum of $CuFeO_2$ nanosheet, $CuFeO_{2+\delta}$ nanosheet and $CuFeO_{2+\delta}$ 2D Janus Layer. Compared with $CuFeO_2$, the presence of excess oxygen has no significant influence on the absorption intensity in the range of 300-1050 nm. But the absorption edge is gradually red-shifting, as increase the content of excess oxygen. In the range of 1050-1500 nm and 1500-2600 nm, the absorption intensity is obviously enhanced, especially in the later range, which is mainly due to the formation of a new impurity level near the Fermi level after the introduction of excess oxygen. This phenomenon is consistent with our previous report. The absorption spectra of $CuFeO_{2+\delta}$ nanosheet and $CuFeO_{2+\delta}$ 2D Janus Layer samples are basically the same, which indicates that $CuFeO_{2+\delta}$ has an intrinsic open layered structure, and the microstructures of $CuFeO_{2+\delta}$ 2D Janus Layer sample are basically the same as $CuFeO_{2+\delta}$ nanosheet, which is

consistent with the data analysis in Fig. 1(a) and the FTIR spectrum analysis in Figure S1 (b).

3. Photocatalytic performance of as-prepared samples

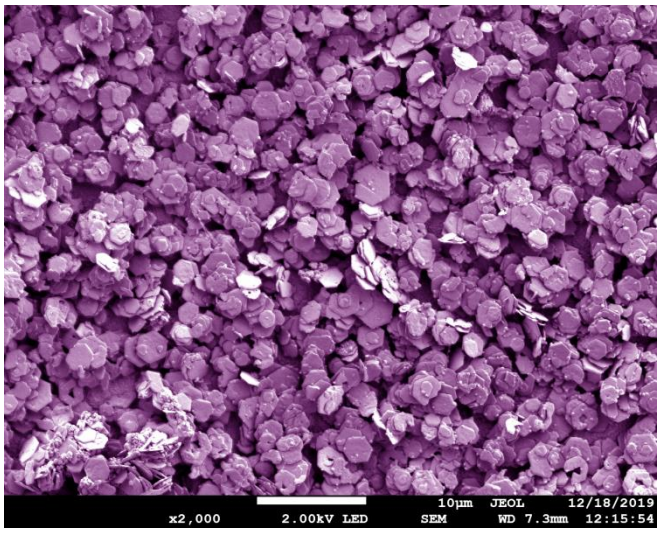

Figure S7. Top-view SEM image of $CuFeO_{2+\delta}$ film prepared by drop-casting method.

Electrochemical characterizations were performed using $CuFeO_{2+\delta}$ powders prepared as film-based electrode. The SEM image of Figure S7 provides a top-view of $CuFeO_{2+\delta}$ film prepared by drop-casting and annealing treatment. Since the film was annealed at 400 ℃ in an air atmosphere for two hours, a small amount of the hexagonal nanosheets in the film were destroyed. Due to the above reasons, in addition to the morphology of a large number of hexagonal nanosheets, there is also a small number of damaged irregular morphology in the SEM image. However, their proportion is very small and will not have a significant impact on subsequent tests.

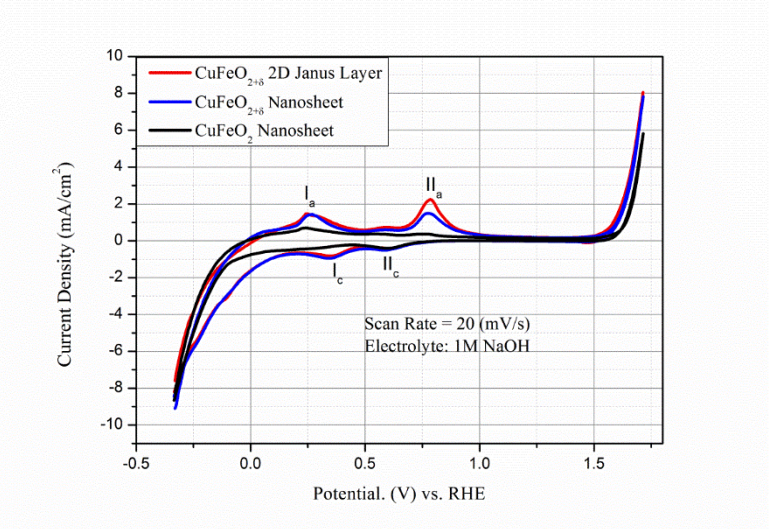

Figure S8. Cyclic voltammetry curve of as-prepared $CuFeO_2$ Nanosheet，$CuFeO_{2+\delta}$ Nanosheet, and $CuFeO_{2+\delta}$ 2D Janus Layer

Figure S8 is the cyclic voltammetry curve of $CuFeO_2$ Nanosheet，$CuFeO_{2+\delta}$ Nanosheet, and $CuFeO_{2+\delta}$ 2D Janus Layer three thin film samples. The redox peaks and corresponding currents of $CuFeO_{2+\delta}$ 2D Janus Layer is the most notable, suggesting the presence of single-/few- layer $CuFeO_{2+\delta}$ can speed up the redox reaction. According to the reported data, these redox peaks can be assigned to some active species couples, which are listed in Table S1. The presence of these active species and the increased current density indicate that the presence of excess oxygen can enhance the activity of hydrogen evolution reaction (HER) of the electrodes from water-splitting.

Table S1. Identified peaks on the CV of in Figure S8, in which the values are referred to Ref. [4]

Peak	Redox process	Potential (V) vs. RHE
I_a	Cu(0) - Cu(I)	0.259
II_a	Cu(I) - Cu(II)	0.785
I_c	Cu(I) - Cu(0)	0.346
II_c	Cu(II) - Cu(I)	0.586

Table S2. Fitting parameters of equivalent circuit in Fig. 4(c)

Sample	R_Ω /Ω	R_{ct} /Ω	C_d /10^{-4} F
$CuFeO_2$ Nanosheet	4.402	877.9	2.15
$CuFeO_{2+\delta}$ Nanosheet	5.458	861.1	2.14
$CuFeO_{2+\delta}$ 2D Janus Layer	4.283	327.5	2.97

4. Photocatalytic degradation testing of 3R-delafossite $CuFeO_{2+\delta}$ samples

As-prepared $CuFeO_2$ nanosheet/$CuFeO_{2+\delta}$ nanosheet/$CuFeO_{2+\delta}$ 2D Janus Layer powders (0.1 g) were dispersed in 100 mL solution of 20 mg/L hydrochloride tetracycline (TCH), followed by adjusting temperature to 10 ℃. The suspension was mechanically stirred in dark for 45 min to achieve the adsorption/desorption balance between the TCH solution and the $CuFeO_2$ nanosheet/$CuFeO_{2+\delta}$ nanosheet/$CuFeO_{2+\delta}$ 2D Janus Layer powders. After the reaction was started, solution samples (3.0 mL) were taken every 15 min, and centrifuged at 7,000 rpm for 10 min on a centrifugal (KAIDA KH23A, China) to remove $CuFeO_2$ Nanosheet, $CuFeO_{2+\delta}$ Nanosheet, $CuFeO_{2+\delta}$ 2D Janus Layer powder samples. The concentration of TCH in the supernatant was determined by UV-Visible spectrophotometer (Hitachi U3900H, Japan). All measurements were repeated three

times and the results were reproducible within the experiments errors.

In fact, the TCH degradation experiments of the three samples used the same prepared TCH solution, that is, their initial concentrations are exactly the identical. From the previous BET measurements, we know that the specific surface areas of the three samples are quite different, which means that their adsorption capacity for TCH will also be quite different. In order to show the difference of TCH adsorption and degradation capacity of the three samples at the same time in Figure S9, we set the time when the light source is turned on to t = 0, and the TCH concentration corresponding to this time to C_0. There is no light illumination in the time range from t = - 45 to t = 0 m, that is, the adsorption-desorption stage of TCH by three samples. It can be seen from Figure S9, when t = - 15 m, the concentration of TCH does not change, meaning that the adsorption-desorption equilibrium has been reached. Due to the different adsorption capacity of TCH for the three samples, the concentration value C_0 of TCH solution added to the three samples at t = 0 is different. Therefore, back calculation shows that the C/C_0 of TCH solution added to three samples is different, when t = -45 m ($CuFeO_2$ Nanosheet, $CuFeO_{2+\delta}$ Nanosheet, and $CuFeO_{2+\delta}$ 2DJanus Layer samples are 1.345, 2.815, and 10.204, respectively). Their difference reflects the difference of adsorption capacity. So, the adsorption capacity of $CuFeO_{2+\delta}$ 2DJanus Layer sample for TCH is 7.6, 3.6 times than that of $CuFeO_2$ Nanosheet and $CuFeO_{2+\delta}$ Nanosheet samples. After turning on the light source, the as-prepared $CuFeO_{2+\delta}$ 2DJanus Layer sample can almost completely photocatalytic degrade TCH within 30 minutes, so its photocatalytic degradation ability is the strongest.

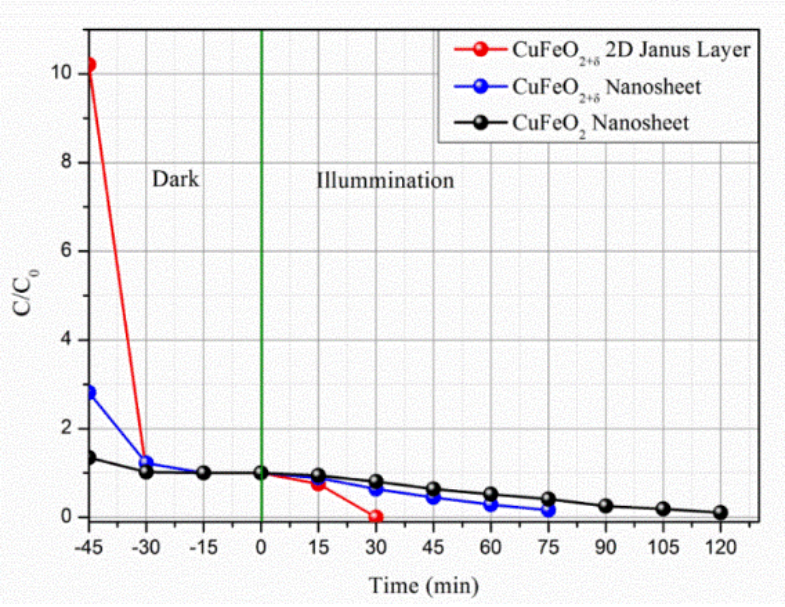

Figure S9. The degradation behaviors of TCH by as-prepared $CuFeO_2$ Nanosheet, $CuFeO_{2+\delta}$ Nanosheet, and $CuFeO_{2+\delta}$ 2DJanus Layer samples under conditions of pH ≈ 7.0, T = 10 ˚C.

5. Electronic structure of 2D Janus $CuFeO_{2+\delta}$ Single-layer

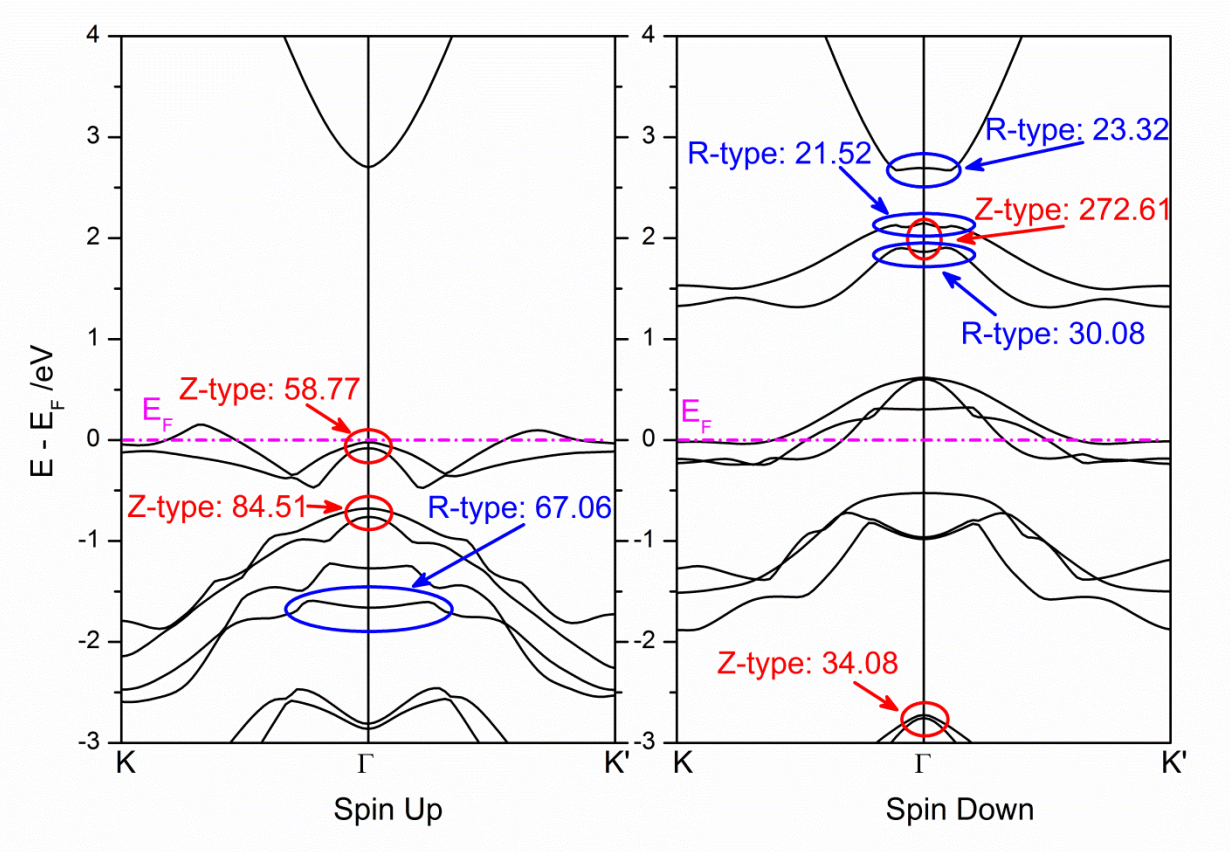

Figure S10. The Spin-Orbit Coupling (SOC) band structure of 2D Janus $CuFeO_{2+\delta}$ Single-layer: The red circle indicates the Zeeman-type (i.e. Z-type) spin-splitting; the blue circle indicates the Rashba-type (i.e. R-type) spin-splitting. The unit of spin-splitting energy is meV.

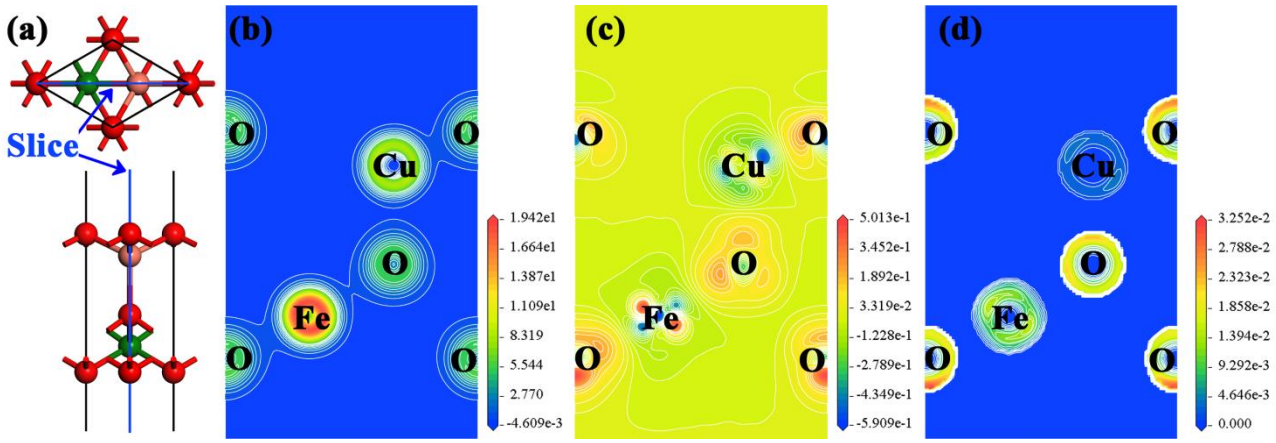

Figure S11. (a) The position of slice in the model of 2D Janus $CuFeO_{2+\delta}$ Single-layer; (b) electron density, (c) electron density difference, and (d) electron localization function maps of 2D Janus $CuFeO_{2+\delta}$ Single-layer at the slices in (a).

Table S3. The Mulliken populations of $CuFeO_2$, $CuFeO_{2+\delta}$, and $CuFeO_{2+\delta}$

Materials	Atomic Populations /e			Bond Populations /e	
	Cu	Fe	O	Cu-O	Fe-O
$CuFeO_2$	0.31	1.14	-0.73	0.28	0.79
$CuFeO_{2+\delta}$	0.69	1.15	O_{Cu}: -0.58 O_m: -0.66 O_{Fe}: -0.58	Cu-O_{Cu}: 0.92 Cu-O_m: 0.14	Fe-O_{Fe}: 0.80 Fe-O_m: 0.86
2D Janus $CuFeO_{2+\delta}$ Single-layer	0.81	1.06	O_{Cu}: -0.65 O_m: -0.65 O_{Fe}: -0.61	Cu-O_{Cu}: 0.83 Cu-O_m: 0.12	Fe-O_{Fe}: 0.79 Fe-O_m: 0.79

O_{Cu}: the O atom is bonded to Cu atom; O_m: the O atom is located at the middle of single-layer; O_{Fe}: the O atom is bonded to Fe atom

Reference

1. Liu, Q.-L.; Zhao, Z.-Y.; Zhao, R.-D.; Yi, J.-H., Fundamental Properties of Delafossite $CuFeO_2$ as Photocatalyst for Solar Energy Conversion. *Journal of Alloys and Compounds* **2020**, *819*, 153032.
2. Liu, Q.-L.; Zhao, Z.-Y.; Yi, J.-H., Excess Oxygen in Delafossite $CuFeO_{2+\delta}$: Synthesis, Characterization, and Applications in Solar Energy Conversion. *Chem. Eng. J.* **2020**, *396*, 125290.
3. Wang, M.; Liu, C.; Shi, H.; Long, T.; Zhang, C.; Liu, B., Facile Synthesis of Chitosan-Derived Maillard Reaction Productions Coated $CuFeO_2$ with Abundant Oxygen Vacancies for Higher Fenton-Like Catalytic Performance. *Chemosphere* **2021**, *283*, 131191.
4. Abd El Haleem, S. M.; Abd El Aal, E. E., Electrochemical Behavior of Copper in Alkaline-Sulfide Solutions. *Corrosion* **2006**, *62*, 121-128.